International Journal of Nanomedicine

Dovepress

open access to scientific and medical research

Open Access Full Text Article

ORIGINAL RESEARCH

Synergistic Effect of Layered Double Hydroxides Nanodosage Form to Induce Apoptosis and Ferroptosis in Breast Cancer

Siyan Pang[1,2], Chenchen Geng[1,2], Zihan Fan[2], Min Hou[1,3], Huilan Mao[1,2], Shuang Tao[1,4], Jing Wang[1,4], Yulun Wu[1,2], Ke Wei[1,4], Yunhao Li[1,2], Liuyang Yan[1,2], Qingling Yang[1,4,5], Changjie Chen[1,4,5], Wenrui Wang[1,2,6]

[1]Anhui Province Key Laboratory of Translational Cancer Research, Bengbu Medical University, Anhui, People's Republic of China; [2]Department of Life Sciences, Bengbu Medical University, Anhui, People's Republic of China; [3]School of Basic Courses, Bengbu Medical University, Anhui, People's Republic of China; [4]Clinical Testing and Diagnose Experimental Center, Bengbu Medical University, Anhui, People's Republic of China; [5]Department of Biochemistry and Molecular Biology, Bengbu Medical University, Anhui, People's Republic of China; [6]Department of Biotechnology, Bengbu Medical University, Anhui, People's Republic of China

Correspondence: Wenrui Wang; Changjie Chen, Anhui Province Key Laboratory of Cancer Translational Medicine, Bengbu Medical University, 2600 Donghai Avenue, Bengbu, Anhui, 233030, People's Republic of China, Email wenrui-wang1983@163.com; tochenchangjie@163.com

Background: Breast cancer is the most common cancer in women and one of the leading causes of cancer death worldwide. Ferroptosis, a promising mechanism of killing cancer cells, has become a research hotspot in cancer therapy. Simvastatin (SIM), as a potential new anti-breast cancer drug, has been shown to cause ferroptosis of cancer cells and inhibit breast cancer metastasis and recurrence. The purpose of this study is to develop a novel strategy boosting ferroptotic cascade for synergistic cancer therapy.

Methods: In this paper, iron base form of layered double hydroxide supported simvastatin (LDHs-SIM) was synthesized by hydrothermal co-precipitation method. The characterization of LDHs-SIM were assessed by various analytical techniques, including ultraviolet-visible (UV-vis) spectroscopy, X-ray diffraction (XRD), Fourier transform infrared (FTIR) spectroscopy, and transmission electron microscopy (TEM). Biological activity, ferroptosis mechanism and biocompatibility were analyzed through in vivo and in vitro analysis, so as to evaluate its therapeutic effect on breast cancer.

Results: The constructed LDHs-SIM nanosystem can not only release SIM through mevalonate (MVA) pathway, inhibit the expression of glutathione peroxidase 4 (GPX4), inhibit the expression of SLC7A11 and reduce the synthesis efficiency of GSH, but also promote the accumulation of Fe^{2+} in cells through the release of Fe^{3+}, and increase the intracellular ROS content. In addition, LDHs-SIM nanosystem can induce apoptosis of breast cancer cells to a certain extent, and achieve the synergistic effect of apoptosis and ferroptosis.

Conclusion: In the present study, we demonstrated that nanoparticles of layered double hydroxides (LDHs) loaded with simvastatin were more effective than a free drug at inhibiting breast cancer cell growth, In addition, superior anticancer therapeutic effects were achieved with little systemic toxicity, indicating that LDHs-SIM could serve as a safe and high-performance platform for ferroptosis −apoptosis combined anticancer therapy.

Keywords: layered double hydroxides, apoptosis, ferroptosis, simvastatin, breast cancer

Introduction

Breast cancer is the most common cancer in women and one of the leading causes of cancer death worldwide.[1,2] In addition to surgical intervention, chemotherapy is still considered to be the main strategy for clinically effective treatment.[3,4] However, due to chemotherapy resistance and lack of treatment options, the prognosis of patients is still not ideal, so new treatment options still need to be continuously explored. In recent years, ferroptosis has been studied as a novel and effective cancer treatment strategy, and there are many studies in the treatment of breast cancer.[5–8] Ferroptosis is a newly discovered type of programmed cell death with a distinguishing feature from apoptosis, necrosis, and autophagy. Cells exhibit

Received: 17 December 2023
Accepted: 29 April 2024
Published: 13 May 2024

morphological features such as marked mitochondrial wrinkling, reduced mitochondrial cristae, and increased membrane density during ferroptosis, as well as biochemical features such as iron-dependent accumulation of lipid peroxides and reactive oxygen species.[9–11] Ferroptosis and its regulatory proteins, such as glutathione peroxidase 4 (GPX4) and solute carrier family 7 member 11 (SLC7A11), have been reported to play a crucial role in the treatment of breast cancer.[12,13] Drugs have been shown to increase the effect of a high ferroptosis environment on cellular ferroptosis by interfering with iron regulation (eg, expression of iron transport proteins and membrane iron transport proteins) and ferroptosis defense-related (eg, GPX4) expression.[14,15] In conclusion, increasing the ferroptosis content in combination with therapeutic drugs can be a vital reference option for treating breast cancer using ferroptosis effects.

Statins, or 3-hydroxy-3-methyl glutaryl coenzyme A (HMG-CoA) reductase inhibitors, are widely used in the clinical treatment of hyperlipidemia. They significantly reduce HMG-CoA reductase activity through competitive inhibition and inhibit cholesterol synthesis via the mevalonate (MVA) pathway.[16,17] In addition, isopentyl pyrophosphate has been linked to the biosynthesis of GPX4 via the MVA pathway, and HMGCR is involved in the synthesis of isopentyl pyrophosphate.[18,19] Simvastatin (SIM) is a lipophilic statin with antitumor effects in cancer cells in vitro and in vivo, including breast, colon, and prostate.[20] SIM demonstrated potent toxic effects on human breast cancer MCF-7 and MDA-MB-231 cell lines in breast cancer studies; and the mechanism of action of SIM-induced apoptosis in cancer cells has been studied in numerous studies, demonstrating its potential as a new anti-breast cancer drug candidate.[21,22] However, statins are rapidly metabolized, and few drugs accumulate at the lesion site, severely limiting treatment effectiveness. As nanoscale materials are studied further, they are primarily used as drug delivery carriers to improve efficacy. As a result, there is a pressing need to create novel nanomedicines to improve therapeutic statin accumulation.

Layered double hydroxides (LDHs) are positively charged alkaline inorganic nanomaterials composed of divalent and trivalent metal cations covalently bonded to hydroxyl groups, with water molecules and interchangeable anions compensating for the charge balance on the main laminate between the layers. The rich tunability of LDHs composition and structure and host-guest interactions make it possible to create novel LDHs nanocomposites. The traditional ion combination is Mg-Al-LDHs, but the current proposal uses Mg-Fe-LDHs to boost intracellular Fe^{2+}-induced ferroptosis by introducing Fe^{3+} into the tumor microenvironment. As nano-delivery carriers, LDHs have good biocompatibility and biodegradability, slow-release properties, pH-sensitive controlled release characteristics, a relatively inexpensive and environmentally friendly manufacturing process, and distinct advantages in vitro drug delivery.[23,24]

As a type of programmed cell death, ferroptosis differs from apoptosis. Herein, to investigate whether the combination of both cell death pathways contributes to an improvement in the efficacy of cancer treatment, we have designed Mg-Fe-LDHs-Simvastatin that can simultaneously cause tumor cell apoptosis and ferroptosis. This NP was composed of Simvastatin and Mg-Fe-LDHs which could be used to deliver SIM and iron ions to the tumor site at the same time (Scheme 1). The LDHs-SIM could home in the tumor and disassemble under the acidic lysosomal environment in tumor cells to release drugs and iron ions. In addition, LDHs-SIM could induce apoptosis of breast cancer cells to a certain extent, and achieve the synergistic effect of apoptosis and ferroptosis. As a result, a notable antitumor therapeutic effect was achieved via the combination of apoptosis and ferroptosis, suggesting that forming the Mg-Fe-LDHs-Simvastatin delivery system is a promising strategy to fight against tumors.

Material and Methods

Materials, Cell Line, and Animal Model

$MgCl_2$-$6H_2O$ (97%), $FeCl_3$-$6H_2O$ (97%), NaOH (97%), and SIM were purchased from Aladdin Reagent Co., Ltd. (Shanghai, China). DMEM (high sugar) and fetal bovine serum (FBS) were obtained from Thermo Fisher Biochemical Products Co. Beijing, China). Dimethyl sulfoxide (DMSO), cell counting kit-8 (CCK-8), Annexin V-FITC/PI, BCA protein assay, SDS-PAGE, GSH kit was purchased from Solarbio (Beijing, China), ROS assay kit was purchased from Beyotime (Nanjing, China). C11 BODIPY 581/591 Lipid Peroxide Fluorescent Probes were purchased from ABclonal (Wuhan, China). Antibodies used in the experiments included HMGCR (1:1000), Bcl-2 (1:1000) purchased from ABclonal (Wuhan, China), BAX (1:1000), GPX4 (1:1000) purchased from Proteintech (Wuhan, China), SLC7A11 (1:1000), β-actin (1:10,000), Horseradish peroxidase (HRP)-labeled goat anti-rabbit antibody (1:6000) was purchased

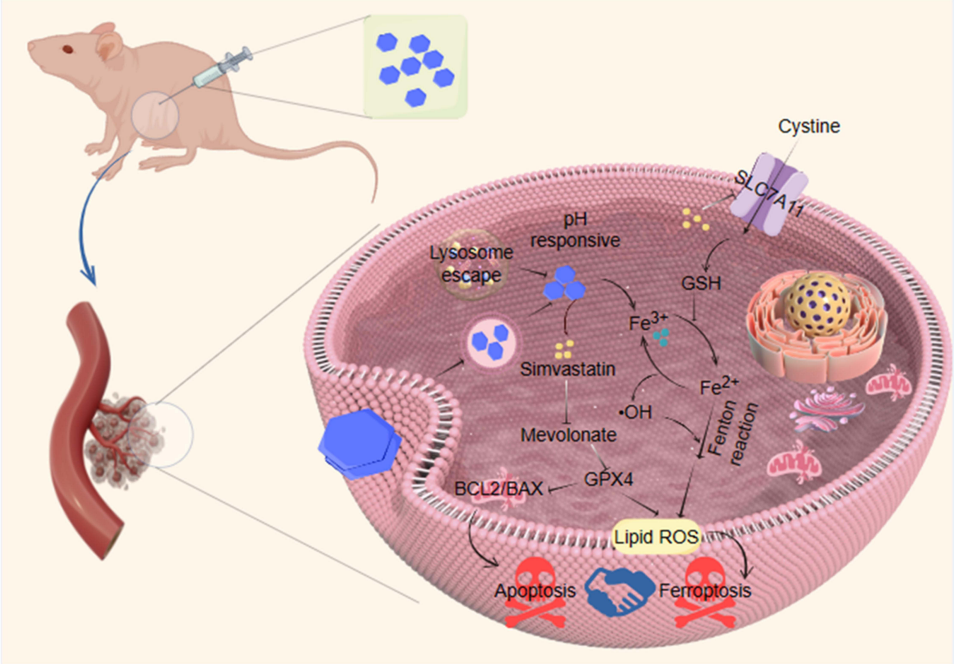

Scheme 1 Schematic illustration of the Mg-Fe-LDHs-SIM nanodrug delivery system in the treatment of breast cancer. LDHs-SIM is ingested by breast cancer cells, Fe^{3+} can be dissociated and cells can produce a large amount of ·OH, resulting in the increase of ROS level. The released SIM from LDHs-SIM inhibits GPX4 expression through MVA pathway. At the same time, SIM can inhibit the expression of SLC7A11 and then reduce the level of GSH in cells, leading to the occurrence of ferroptosis.

from Affinity Biosciences (Nanjing, China). The Ferro Orange kit was purchased from Dojindo laboratories (Shanghai, China).

The human breast cancer cell line MDA-MB-231 and SKBR3 were purchased from the Chinese Academy of Sciences (Shanghai, China) and maintained in complete DMEM supplemented with 10% fetal bovine serum, 1% penicillin and 1% streptomycin at 37°C and 5% CO_2. The MCF10A was purchased from Procell, Wuhan, China. MCF10A cells were maintained as monolayers in DMEM medium supplemented with 5% horse serum, 0.2% EGF (20mg/mL), hydrocortisone (0.5mg/mL), insulin (10 μg/mL), 100U/mL penicillin, and 100μg/mL streptomycin at 37°C in a humidified incubator with 5% CO_2. Female BALB/c nude mice (5 weeks old) were purchased from Changzhou Cavins Laboratory Animal Co., Ltd. (license number: SCXK SU 2021–0013), and were housed in a SPF animal room at 25°C, with relative humidity maintained at 40% - 70%. All animal experiments were conducted with approval from the Bengbu Medical University Institutional Animal Care and Use Committee (Ethics Number: [2023] No. 537). All animal experiments were performed in accordance with the "Guidance for the Care and Use of Laboratory Animals".

Preparation of Layered Double Hydroxides and Layered Double Hydroxides-Loaded Simvastatin

LDHs were synthesized by hydrothermal and co-precipitation techniques. Calculate the mass of magnesium chloride ($MgCl_2$•$6H_2O$) and iron chloride ($FeCl_3$•$6H_2O$) according to the molar ratio of Mg^{2+} to Fe^{3+} of 3:1, and prepare 10 mL of the mixed metal salt solution. Prepare 40 mL of alkali solution configured with NaOH. Add the alkali solution under nitrogen atmosphere at 37°C and adjust the pH to 10 ± 0.01 by adding the salt solution dropwise while stirring. The mixture was then incubated in a water bath for 0.5 hours. After centrifugation, the supernatant was discarded to obtain out initial product. The initial precipitation product of LDHs was resuspended in 40 mL of deionized water and reacted in a hydrothermal reactor at 100°C for 16 h, and then allowed to cool. After centrifugation at 7600 rpm for 10 min, the cells were washed twice with deionized water, and the resulting 10 mL of LDHs suspension was resuspended in deionized water and lyophilized in a lyophilizer and set aside. (The deionized water used in the synthesis process has had the carbon dioxide removed).

LDHs-SIM was also synthesized by hydrothermal and co-precipitation techniques. Prior to mixing the solutions, all solutions were heated to 60 °C with nitrogen gas bubbling for 20 min. A solution of NaOH (40 mL, 0.15 M) and a mixed solution (10 mL) containing $MgCl_2$•$6H_2O$ (0.3 M) and $FeCl_3$•$6H_2O$ (0.1 M) were added dropwise to a drug solution (10 mL,0.1 M) containing simvastatin (SIM) sodium, at 60 °C with nitrogen gas purging. The mixture was continuously stirred for 6 min at 60 °C under N_2 gas purging. The resulting mixture was separated, washed and dispersed in 40 mL deionized water.

Characterization

A drop of dilute solution of LDHs and LDHs-SIM was placed on a carbon-coated copper TEM grid. The samples were imaged using a JEM-1230 transmission electron microscope and observed under a microscope at 120 kV. The particle size and polydispersity index at 25°C were determined by photon correlation spectroscopy. Zeta potential values were estimated from the electrophoretic mobility at 25°C using the same equipment. The colloidal stability of LDHs and LDHs-SIM in PBS was investigated. Fourier transform infrared spectroscopy (FT-IR) was used to identify the structure and chemical composition of LDHs and LDHs-SIM nanopreparations. Measurements were performed on a Bruker Vector 22 FT-IR spectrophotometer in the range of 400 to 4000 cm^{-1}. X-ray powder diffraction (XRD) patterns were measured on a Rigaku Miniflex diffractometer using Cu Kα radiation (λ = 1.54060 Å, 40 kV, 40 mA, step of 0.0330°) recorded from 5° to 80°. UV absorption were performed using a spectrophotometer (UV, 3100, Hitachi, Japan).

Drug Loading of LDHs-SIM

The content of SIM in LDHs-SIM was determined by UV-VIS absorption spectrometry. SIM solutions with concentrations of 0.5, 1, 2, 4, 8 and 16 μg/mL were prepared in methanol, and their absorbance at 238 nm was determined. The standard curve of the absorbance-concentration of SIM in methanol was obtained. Take 5mg LDHs-SIM dry powder and dissolve it in 3 mL methanol. Then methanol was added to the final volume of 10 mL and ultrasonic suspension was performed. Then, the concentration of SIM was determined by measuring the absorbance at λmax = 238 nm by ultraviolet spectrophotometer, and the drug loading of LDHs-SIM was calculated according to the formula.

Drug Release of LDHs-SIM Under Different pH

Weighed 4mg LDHs-SIM powder into 15 mL centrifuge tube, added 8 mL PBS (pH= 6.2) and 8 mL PBS (pH=7.4) respectively, and shocked them in a shaker at 37 ° C, 100 rpm. At 10, 20, 30, 60, 120, 180, 240 and 360 minutes, 1.5 mL of PBS was taken out and the corresponding absorbance was detected with an ultraviolet spectrophotometer, and an equal amount of fresh PBS was added. The release rate was calculated by comparing simvastatin standard curve and LDHs-SIM loading.

In vitro Cellular Uptake Analysis

2 mg of LDHs-SIM and 2 mg of FITC were dissolved in 1 mL of pure water and mixed with ultrasound for 30 min. Then, the mixture was placed on a shaker at 4°C with low-speed shaking overnight. The next day, the mixture was centrifuged at 3000 rpm/min for 5 min and repeated three times to obtain LDHs-SIM-FITC, and freeze-dried and set aside.

5×10^3 MDA-MB-231 and SKBR3 cells were inoculated into 24-well plates (14 mm, Solarbio, China) and treated with 2.5 μM LDHs-SIM-FITC at different time points (1, 4, 12, 24, and 48 h), respectively. The cell plates were washed twice with PBS and the cells were fixed. The results were observed with a confocal laser scanning microscope (CLSM).

Lysosomal Escape Experiments

Lysosomal escape experiments using FITC fluorescently labeled LDHs-SIM. Seed 1×10^4 cells in each glass bottom cell culture dish, and after the cell adherent morphology is unfolded, change the medium to a dosing solution (prepared with complete medium) with a final concentration of 5μM LDHs-SIM, configure 50 nM Lyso-tracker Red probe solution and pre-incubate to 37°C and incubate for 2 h protected from light. Cells were washed with PBS, and 10 μg/mL Hoechst

solution was added to incubate in the dark for 10~15 min, and the cells were cleaned with PBS. Photographed under a ZEISS fluorescence microscope.

Lysosomal membrane permeability was determined using AO (Acridine Orange) staining solution: 1×10^4 cells were seeded in each glass bottom cell culture dish, 5 μM LDHs-SIM dosing solution was added after cell adherence morphology was unfolded, the liquid in the dish was discarded after incubation for 48 h, and an AO staining solution (complete medium dilution) at a final concentration of 10 μg/mL was added and incubated for 15 min protected from light. Cells were washed with PBS, 400 μL of 4% paraformaldehyde was added to each dish, and after fixation for 15 min, the cells were cleaned with PBS, and the green (Em=490 nm, Ex=528 nm) and red (Em=555 nm, Ex=617 nm) fluorescence channels were observed under a laser confocal microscope.

Cell Proliferation Assay

The effect of different concentrations of SIM and LDHs-SIM on the viability of MDA-MB-231, SKBR3 cells and MCF10A was examined by CCK-8 assay. MDA-MB-231, SKBR3 cells and MCF10A were uniformly inoculated in 96-well plates at a density of 5×10^3 cells per well and grown in 200 μL DMEM medium for 24 hours. Then the cells were incubated in fresh medium (200 μL /well) containing SIM (2.5 μM, 5 μM, 10 μM), LDHs-SIM (2.5 μM, 5 μM, 10 μM) and LDHs, respectively. The absorbance values were measured at 450 nm to detect cell viability.

Measurement of Intracellular Fe^{2+} Content

Ferro Orange is a divalent ferroptosis detection probe that allows fluorescent imaging of Fe^{2+} in living cells. Cells were inoculated in confocal dishes and incubated overnight at 37°C in a 5% CO_2 incubator. The supernatant was discarded and the medium containing the drug was replaced and continued for 48 hours. The medium was discarded, washed once with PBS, Ferro Orange working solution at a concentration of 1 μmol/L was added according to the manufacturer's instruction, incubated at 37°C in a 5% CO_2 incubator, and the results were observed with a live cell imaging system (Axio Observer Z1, Germany ZEISS).

GSH Assay

MDA-MB-231 and SKBR3 cells were inoculated into six-well plates at a density of 1.5×10^5 per well and cultured for 24 hours. Then the medium was discarded and the PBS was washed over, DMEM, LDHs, SIM and LDHs-SIM were added correspondingly and incubated for 48 hours. No less than 5×10^6 cells were collected in each group and the GSH content was calculated according to the Solarbio GSH test kit instructions.

Lipid Peroxidation (LPO) and Reactive Oxygen Species (ROS) Generation

Cells are seeded in six-well plates for 24 hours, replaced with corresponding drug solution for 48 hours, digestion collection cells are centrifuged to obtain pellets, C11-BODIPY (LPO probe) and DCFH-DA (ROS probe) solutions are configured, resuspended and incubated using probe solution, and cell production LPO and ROS are detected using flow cytometry (CytoFLEX, Beckman Coulter).

Transmission Electron Microscopy Assay

Briefly, cells treated with LDHs-SIM for 48 h were collected and fixed with 2.5% glutaraldehyde. After washing twice with PBS, the cells were fixed with 1% pre-cooled osmium tetroxide for 1 hour, then dehydrated with gradient ethanol, incubated with acetone and embedding agent (1:1) at 37°C for 4 hours, ultrafine sectioned by ultra-fine microtome at 70 nm, and transferred to 150 mesh copper film mesh. The sections were stained for 2% uranyl acetate followed by counterstaining for 2.6% lead citrate according to standard staining methods. After drying, the images were scanned using an HITACHI-HT7800 transmission electron microscope (Tokyo, Japan).

Cell Apoptosis

The Annexin V-FITC/PI method was used to detect the effect of LDHs-SIM nanoformulation on apoptosis of MDA-MB-231 and SKBR3 cells. MDA-MB-231 and SKBR3 cells were inoculated into six-well plates and cultured for 24 hours. The medium

was discarded, washed once with PBS, and incubated for 48 h with the corresponding addition of medium, LDHs, SIM, and LDHs-SIM. The cells were then digested with 0.25% trypsin without EDTA and collected. After washing twice with pre-cooled PBS, 500 μL of binding buffer dilution was added. Next, 5 μL of FITC-labeled phospholipid binding protein V (Annexin V-FITC was added) and 5 μL of PI were added and the mixture was well stirred for 15 min at room temperature in the dark. Within 1 h, observation and detection were performed using flow cytometry.

Western Blot Assay

MDA-MB-231 and SKBR3 cells in logarithmic growth phase were inoculated into six-well plates and cultured for 24 h. The original medium was discarded and 2 mL of medium, medium containing LDHs, SIM and LDHs-SIM were added correspondingly. After 48 h of treatment, the groups of cells were collected and protein extracts were prepared in the ratio of 1 mL of cell lysate to 10 μL of phenyl methyl sulfonyl fluoride (PMSF). Protein levels were quantified by the bis quinolinic acid (BCA) method. Protein samples were separated by SDS-PAGE gel electrophoresis, transferred to polyvinylidene difluoride (PVDF) membranes, blocked with skim milk, and incubated with primary and secondary antibodies. Finally, the protein expression of GPX4, HMGCR, SLC7A11, Bcl-2 and Bax in each group was observed on a gel imager (ChemiDoc^{TM}XRS+, Bio-Rad). (The primary antibody dilution ratios used were all 1:1000, Secondary antibody is 1:1000).

Treatment of Tumor-Bearing Mice

The xenograft tumor model is generated by subcutaneous injection of 5×10^5 SKBR3 cells/100 μL of saline into the right flank region of mice. After 10 days, upon tumor growth to a volume of about 50mm^3, a tumor-bearing model was established. The mice were grouped as follows: The control group, LDHs group, SIM group and LDHS-SIM group. According to the standard SIM injection concentration of 20 mg/kg, the corresponding material concentration was allocated, and the PBS containing LDHs-SIM, LDHs, SIM, and PBS were injected peritumorally (n = 5). The injection frequency was 2 days, and injections were administered for 10 days; the weight and tumor volume were recorded. The tumor volume was calculated according to this formula: tumor volume (mm^3) = 0.5× (length×width^2).

Hematoxylin and Eosin Staining (H&E) and Immunohistochemical (IHC) Analysis

The day after peritumoral injection of drugs for 10 days (Day 11), all mice were sacrificed. The viscera (heart, liver, spleen, lung, and kidney) and SKBR3 breast cancer tissues of the mice were fixed in 4% paraformaldehyde, embedded in paraffin and sliced to a thickness of ≈3 μm. Conventional hematoxylin-Iran Hematoxylin and Eosin (H&E staining) were used to perform routine histopathological analysis. Anti-Ki67 antibody staining was used for Ki67 proliferation detection using the following steps: incubation at 4 °C overnight, followed by washing with PBS, incubation with the secondary antibody (green fluorescence) for 2 h, re-staining with DAPI, washing with PBS, and sealing with glycerol. Similarly, the GPX4 IHC index of tumor tissue was detected. TUNEL apoptosis was detected using a TUNEL Apoptosis Assay Kit. Each section was dripped with 50 μL of detection liquid, incubated at 37 °C for 60 min, and washed with PBS.

Statistical Analysis

All data were presented as mean ± standard deviation (SD). *t*-test was used to compare the differences between the two groups. One-way ANOVA analysis of variance was used to analyze differences among three or more groups. Statistical analysis was performed using the GraphPad Prism 8.0 Software. The significant difference was labeled as *p < 0.05, **p < 0.01, and ***p < 0.001.

Results

Preparation and Characterization of Layered Double Hydroxides and Layered Double Hydroxides-loaded Simvastatin

Figure 1A depicts the preparation process for LDHs and LDHs-SIM using the hydrothermal co-precipitation method. Our findings indicate that LDHs and LDHs-SIM were successfully prepared. First, the average particle sizes of LDHs and

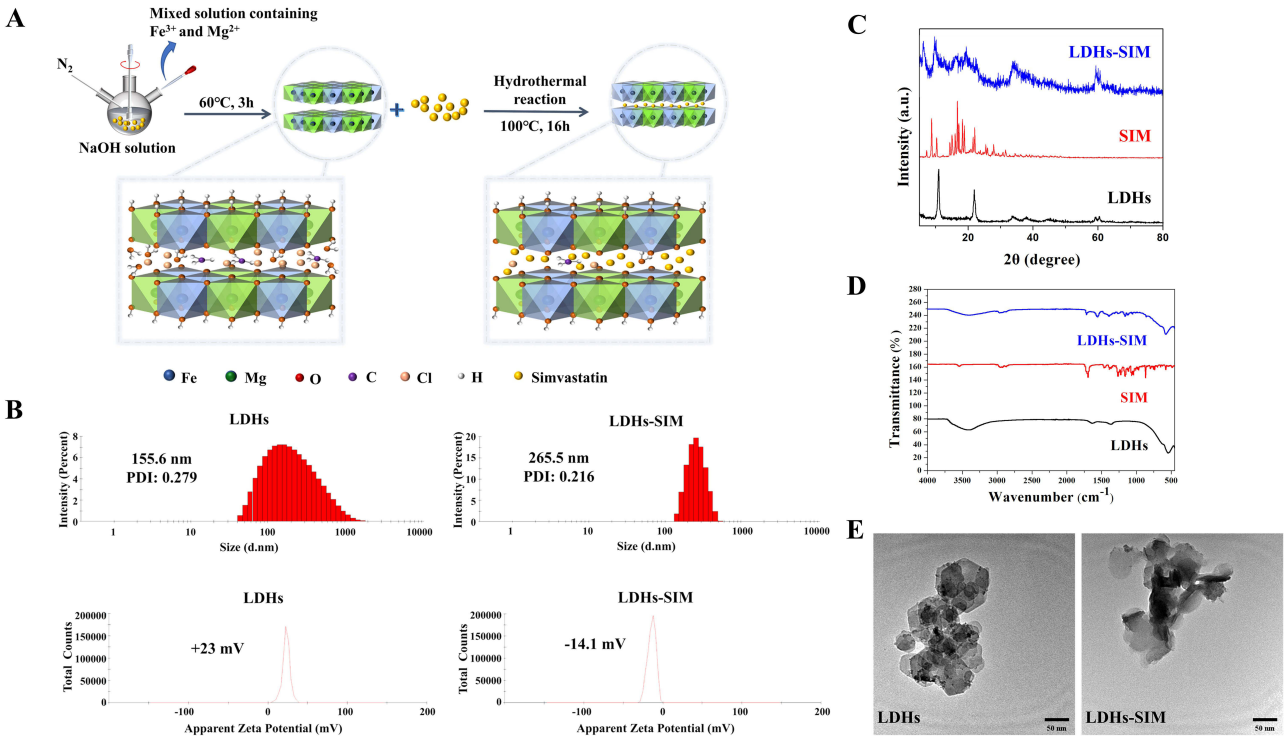

Figure 1 (**A**) Flow chart of LDHs-SIM preparation; (**B**) Size distribution of LDHs and LDHs-SIM, with PDI representing the polymer dispersion index; (**C**) XRD patterns of LDHs, SIM and LDHs-SIM; (**D**) FT-IR spectra of LDHs, SIM and LDHs-SIM; (**E**) TEM images of LDHs and LDHs-SIM at a scale of 50 nm.

LDHs-SIM were 155.6 ± 3.6 nm and 265.5 ± 1.3 nm, respectively, according to dynamic light scattering (DLS). Both particle size distributions were relatively dense, and changes in particle size distribution were consistent with volume changes before and after loading the LDHs drug (Figure 1B). LDHs Zeta potential and LDHs-SIM average potentials were 23.0 ± 1.9 mV and - 14.1 ± 2.1 mV, respectively. The Zeta potential of the LDHs changed from positive to negative before and after SIM loading, most likely due to the drug changing the potential of the carrier (Figure 1B). The drug loading of LDHs-SIM is determined based on the standard curve of SIM (Figure S1), and its drug loading is measured by ultraviolet spectrophotometer. As shown in Table 1, the drug loading of LDHs-SIM is 26.7% ± 1.8%. The presence of characteristic diffraction peaks (003), (006), and (012) for LDHs was shown in Figure 1C, indicating the integrity of their crystal structure. On the other hand, the XRD pattern of LDHs-SIM is flatter, most likely due to drug loading, which results in weaker diffraction peaks. The absorption peaks of the •OH stretching of the adsorbed water molecules in the lamellar structure of LDHs can be seen between 3000 cm^{-1} and 3500 cm^{-1} in the FT-IR pattern (Figure 1D). In addition, the bending vibration of water molecules formed an absorption peak between 1500 cm^{-1} and 2000 cm^{-1}, and the absorption peaks formed between 1000 cm^{-1} and 1500 cm^{-1} and below 800 cm^{-1} were Mg-O and Fe-O bond vibrations in the lattice of LDHs. It indicates that we can use the hydrothermal co-precipitation method to load Mg^{2+} and Fe^{3+} into it. The LDHs-SIM have the characteristic peaks of both LDHs and SIM, and no new chemical bonds are formed, indicating that SIM is successfully loaded into LDHs and is physically bound together. There are no electron micrographs or thermogravimetric results. LDHs carriers are typical hexagonal lamellar wafers with distinct contours and clear dispersion boundaries, as shown in Figure 1E. With the intercalation of simvastatin drug molecules, the morphology of

Table 1 The size, PDI, zeta potential and drug loading og LDHs-SIM

Sample	Size (d. nm)	PDI	Zeta potential (mV)	Drug loading(%) [a]
LDHs	155.6 ± 3.6	0.279 ± 0.03	23.0 ± 1.9	–
LDHs-SIM	265.5 ± 1.3	0.216 ± 0.01	− 14.1 ± 2.1	26.7 ± 1.8

Note: [a]Drug loading% $= \frac{\text{Concentration of SIM in LDHs-SIM}}{\text{Concentration of feeding simvastatin}} \times 100\%$.

nanocomposite particles gradually becomes irregular from regular hexagons, but their sheet structure is visible. Simultaneously, the particle size of nanocomposite particles tends to increase. The percentage of drug release was studied in acidic (pH = 6.2 to simulate the tumor microenvironment: TME) and neutral (pH = 7.4 to simulate physiological conditions) environments. Within 240 minutes, only 46.7% of the drug was released at pH = 7.4, but this percentage increased to 53.5% at pH = 6.2, suggesting that TME may help release the drug (Figure S2).

In vitro Drug Toxicity and Cell Uptake Analysis

CCK-8 experiments revealed that different concentrations of free SIM and LDHs-SIM inhibited the proliferation of MDA-MB-231 and SKBR3 cells for 48 hours. Different concentrations of SIM and LDHs-SIM differed significantly within 48 hours in MDA-MB-231 and SKBR3 cells, as shown in Figure 2A. In contrast, the two breast cancer cells treated with LDHs-SIM showed dose-dependent cytotoxicity as concentrations increased from 2.5 to 10 μM. In order to explore whether SIM and LDHs-SIM have toxic effects on normal breast cells, we selected human breast epithelial cells MCF10A cells and compared them at the same concentration. The results showed that SIM and LDHs-SIM had no toxic effect on MCF10A cells at the selected concentration. Low concentrations (2.5 μM and 5 μM) of SIM have a growth-promoting effect on MCF10A.

We examined the internalization of LDHs-SIM-FITC by MDA-MB-231 and SKBR3 cells by CLSM to confirm successful delivery of LDHs-SIM to target cells. Figure 2B shows that MDA-MB-231 and SKBR-3 can absorb LDHs-SIM in 4 hours and that the fluorescence decreases with time, indicating drug consumption. The location of LDHs-SIM in MDA-MB-231 and SKBR3 breast cancer cells was also investigated. Lyso-Tracker Red is a lysosomal red fluorescent probe that penetrates cell membranes and can be used to stain lysosomes in living cells. As shown in Figure 2C, when cells take up LDHs-SIM, the red lysosomal and green fluorescence overlap, indicating that the nanocarrier can be internalized via the lysosomal pathway. Acridine orange (AO) is a lysosomal metachromatic fluorescent dye that glows red in lysosomes and green in the cytoplasm. As shown in Figure 2D, cells in the control group showed evident red fluorescence. In contrast, cells incubated with LDHs-SIM showed weak red and apparent green fluorescence. It indicates that lysosomal membrane permeability increased after LDHs-SIM treatment, and some AO dyes entered the cytoplasm. In conjunction with lysosomal experimental findings, the mechanism of LDHs-SIM escape from the lysosomal pathway may be that LDHs-SIM can reduce the risk of drug clearance by lysosomes in cells, which is conducive to improving drug delivery efficiency.

In vitro Ferroptosis and Apoptosis Analysis

Ferro Orange was used in cells as a Fe^{2+} detection reagent to investigate the phagocytosis characteristics of nanoparticles and to confirm the transformation of Fe^{3+} to Fe^{2+}. As shown in Figure 3A, when MDA-MB-231 and SKBR3 cells were treated with LDHs and LDHs-SIM, there was apparent orange fluorescence. In contrast, the control and free SIM groups had very little orange fluorescence, indicating that nanoparticles can produce a large amount of Fe^{2+} in cells, which is conducive to the occurrence of the ferroptosis Fenton reaction.[25] According to research, tumor cells have higher levels of H_2O_2 and glutathione than normal cells, while intracellular pH is weakly acidic.[26] Furthermore, the basic nanoparticles LDHs-SIM proposed by us can release Fe^{3+} in slightly acidic tumor cells and be reduced to Fe^{2+} by GSH, resulting in GSH depletion in tumor cells, which is also an essential manifestation of ferroptosis. As shown in Figure 3B, the LDHs and SIM groups significantly inhibited the GSH content of MDA-MB-231 and SKBR3 cells ($p < 0.05$) compared to the control group.

According to some, the lethality of ferroptosis is primarily due to the formation of excess lipid reactive oxygen species.[27] The LPO probe can bind to lipid-reactive oxygen species in cells. LPO content was determined using the fluorescence intensity response lipid reactive oxygen species content, as shown in Figure 3C. The results showed that after LDHs-SIM treatment, the content of LPO in MDA-MB-231 and SKBR3 cells was significantly higher than in the free SIM treatment group ($p < 0.001$).

The Fenton reaction is well known for producing ROS from ferrous ions. We know from the above experiments that LDHs-SIM causes increased Fe^{2+} content in tumor cells. 2,7-dichlorodihydrofluorescein diacetate (DCFH-DA) is used as a fluorescent probe to detect ROS generation and observe ROS generation visually. Flow cytometry was used to detect

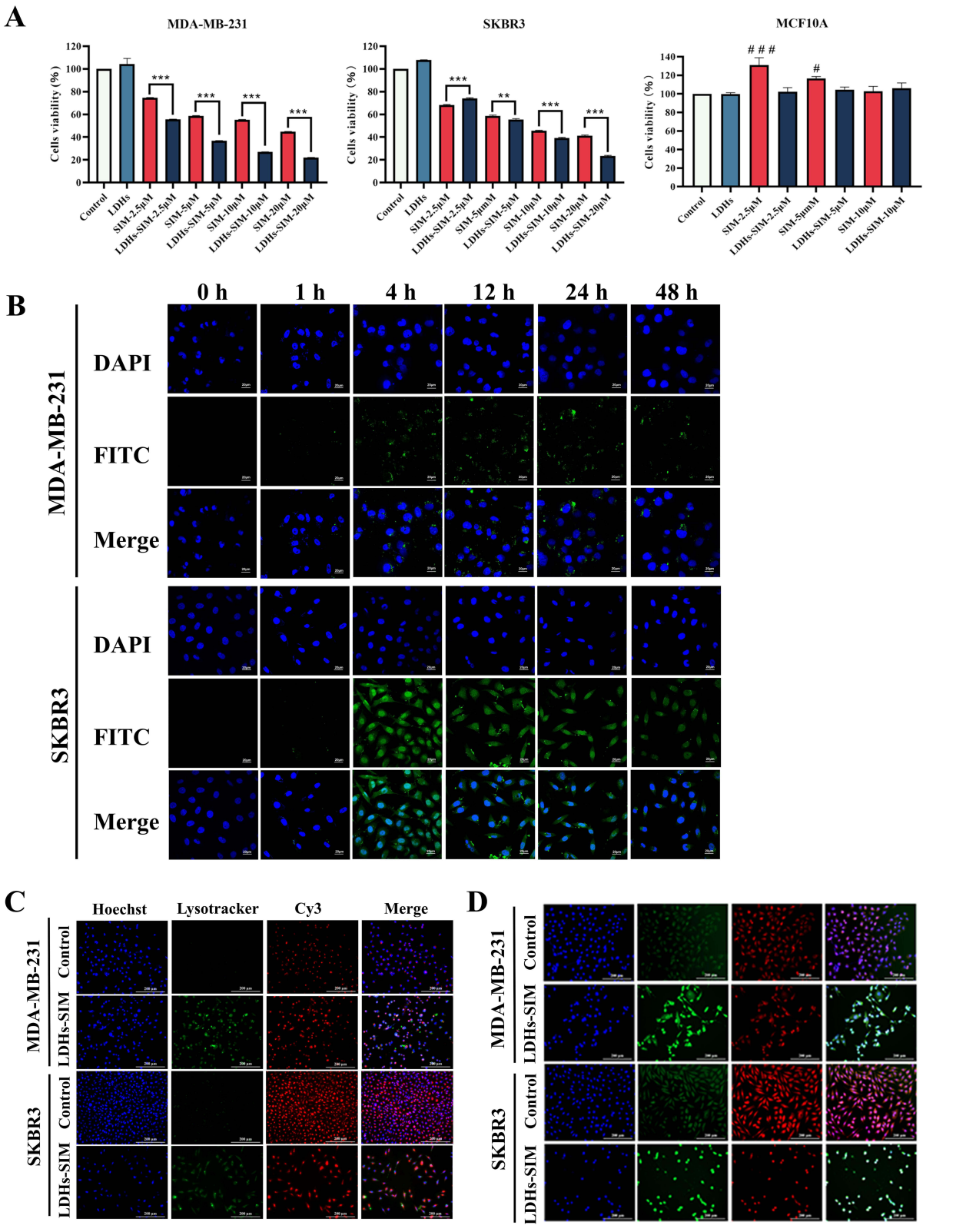

Figure 2 (**A**) The cell viability of MDA-MB-231, SKBR3 and MCF10A after 48 h treatment with LDHs, different concentrations of SIM and LDHs-SIM. (**B**) Confocal images of LDHs-SIM-FITC and nuclei (DAPI) at different time points in MDA-MB-231 and SKBR3 cells, scale bar: 20 μm; (**C**) After 48 h of incubation, localize LDHs-SIM-FITC cells in MDA-MB-231 versus SKBR3 cells and label with Hoechst (blue) and Lyso-tracker Red (red) to distinguish nuclei and lysosomes, respectively, scale bar: 200 μm; (**D**) Acridine Orange staining (green and red fluorescence distribution) for lysosomal membrane permeability, scale bar: 200 μm. Data are expressed as mean ±SD, $^{**}P < 0.01$, $^{***}P < 0.001$. # stands for statistics with Control, $^{\#}P < 0.1$, $^{\#\#\#}P < 0.001$.

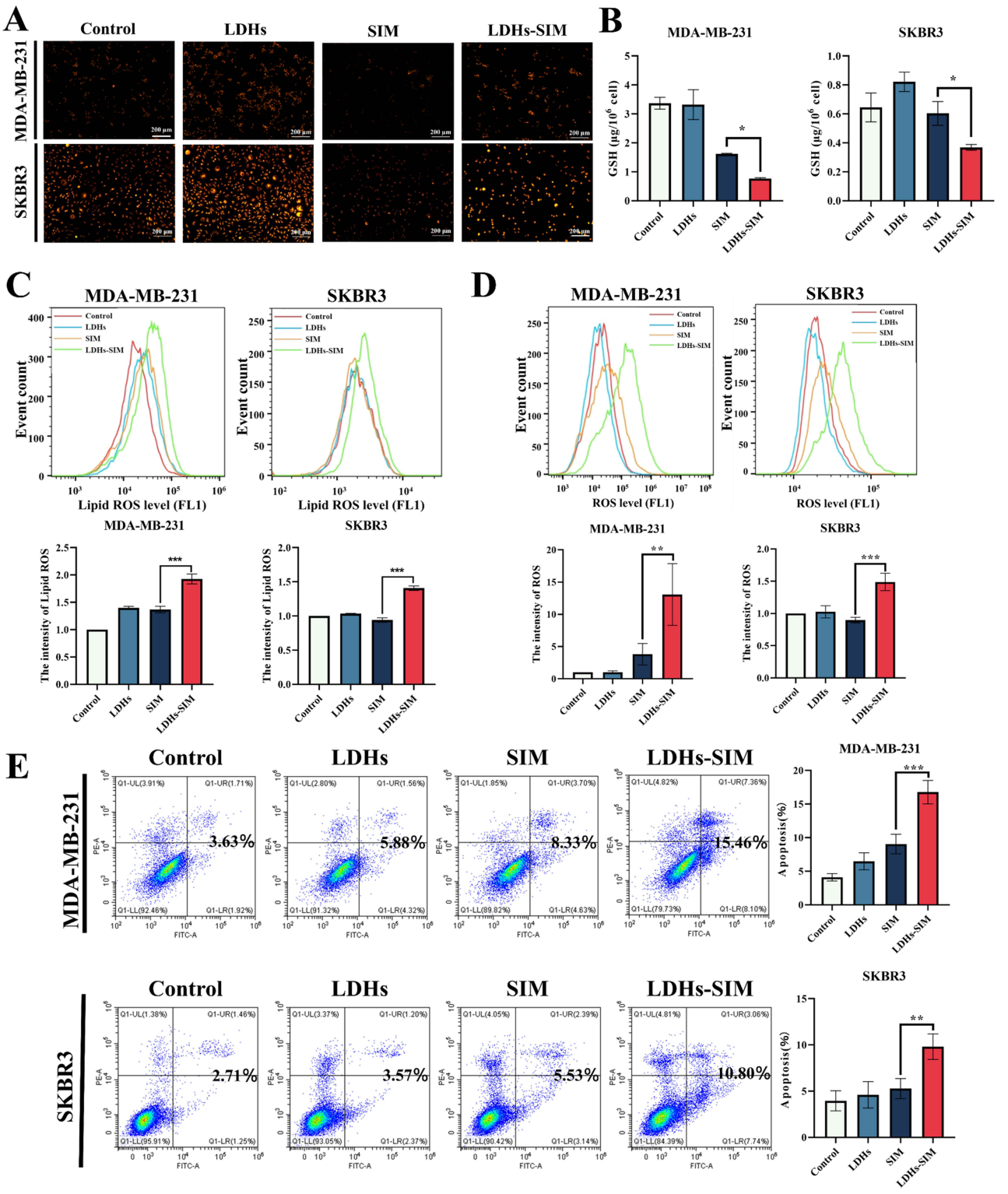

Figure 3 (**A**) Fe^{2+} in each group of MDA-MB-231 and SKBR3 cells taken by live-cell workstation, scale: 200 μm; (**B**) The kit detected the GSH content of each group of MDA-MB-231 and SKBR3 cells after treatment; (**C**) Flow cytometry to detect the LPO content of MDA-MB-231 and SKBR3 cells in each group after drug treatment; (**D**) Flow cytometry to detect the ROS content of MDA-MB-231 and SKBR3 cells in each group after drug treatment; (**E**) Representative images of apoptosis within 48 hours of MDA-MB-231 and SKBR3 cells after treatment with different group. Data are expressed as mean ±SD, *P < 0.05, **P < 0.01, ***P < 0.001.

ROS production in MDA-MB-231 and SKBR3 cells, as shown in Figure 3D, and LDHs-SIM could significantly induce ROS production in cells compared to the SIM-treated group ($p < 0.01$, $p < 0.001$).

SIM and LDHs-SIM can both induce apoptosis in MDA-MB-231 and SKBR3 cells, according to flow cytometry analysis (Figure 3E). According to the apoptosis rate indicated in the figure, in MDA-MB-231 cells, the apoptosis rate of the LDHs-SIM group was about 1.86 times that of the SIM group and 4.26 times that of the Control group; in SKBR3 cells, the apoptosis rate of the LDHs-SIM group was about 1.95 times that of the SIM group and 4 times that of the Control group. LDHs-SIM induces apoptosis more effectively than free drugs ($p < 0.001$, $p < 0.01$).

In addition, we can confirm the presence of ferroptosis by using transmission electron microscopy to examine the morphological changes in MDA-MB-231 and SKBR3 cells. Figure 4A shows that after 48 hours of SIM and LDHs-SIM treatment, cancer cells had increased density of mitochondrial membranes and decreased density of mitochondrial crest compared to the blank-treated group and LDHs, which are typical morphological features of ferroptosis and were most pronounced after LDHs-SIM treatment.

Statins are small molecule inhibitors of 3-hydroxy-3-methylglutaryl-CoA reductase (HMGCR) that can affect the MVA pathway to control cholesterol biosynthesis, inhibiting some metabolites and inactivating GPX4.[28,29] GPX4 is a well-known key indicator for determining whether a cell has ferroptosis. To further investigate LDHs-SIM-induced ferroptosis, we used Western blot to look at the effect of LDHs-SIM on the MVA pathway in MDA-MB-231 and SKBR3 cells. As shown in Figure 4B, adding SIM and LDHs-SIM reduced the expression of GPX4 and HMGCR proteins in MDA-MB-231 and SKBR3 cells compared to the control group. LDHs-SIM was more effective on GPX4 and HMGCR protein expression than the control group. Furthermore, previous research has shown that LDHs-SIM can cause ferroptosis by depleting GSH. SLC7A11 is a key protein in GSH synthesis, so we included it in the study. The results showed that LDHs-SIM can reduce SLC7A11 expression and thus inhibit GSH synthesis.

Therapeutic Effect in vivo

A tumor-bearing mouse model of SKBR3 breast cancer was established and randomly divided into four groups, as shown in Figure 5A: PBS, LDHs, free SIM, and LDHs-SIM. Peritumor injection treatment began at approximately 60 mm^3, and mouse weight and tumor volume were monitored once every two days, during which time tumor growth in different groups of mice was documented using hand-held mouse photographs (Figure 5B) until all mice were sacrificed on day 10 (Figure 5C). Figure 5E shows no significant change in mouse body weight across all treatment groups, indicating that the nanodrug loading system was low toxicity and biologically safe. In Figure 5F, the relative tumor volume of the PBS group increased rapidly due to the malignant growth of SKBR3 tumors, the tumor volume of the LDHs group was no different from that of the PBS group, essentially did not show a therapeutic effect, and the free SIM showed a particular tumor suppressive effect. In contrast, the LDHs-SIM group could effectively reduce tumor growth ($p < 0.001$), show smaller tumor size ($p < 0.05$), and have a lighter tumor weight ($p < 0.01$), indicating that the nanodrug delivery system can effectively inhibit tumors compared to monotherapy. In vitro photographs of tumors and corresponding tumor volumes and weights show synergistic therapeutic effects (Figures 5D, G, and H).

To further confirm the therapeutic effect of LDHs-SIM nanoplatform, hematoxylin and eosin were used to analyze different treated tumor tissues (H&E), TUNEL and Ki67 staining (Figure 6A). From the H&E staining results, it is clear that most pink tumor cells are present in the LDHs-SIM group compared to other treatment groups, indicating that they are effective in damaging tumor tissue. The results of TUNEL showed that the apoptosis rate of mouse tissue in LDHs-SIM was significantly higher than that in other treatment groups. For the Ki67 assay, the lowest positive brownish-yellow signal was detected in the LDHs-SIM group, indicating that they can effectively inhibit tumor proliferation. Immunohistochemical analysis of tumor GPX4 expression in different groups of mice showed that the LDHs-SIM treatment group was significantly lower than that in the free SIM treatment group, which was consistent with the previous results at the cell level (Figure 6A).More importantly, as shown in Figure 6B, the H&E results show that neither LDHs nor LDHs-SIM cause damage to the heart, liver, spleen, lungs and kidneys of mice during the treatment process, indicating that the nanodrug-loaded system has good biocompatibility and has good application prospects in cancer treatment.

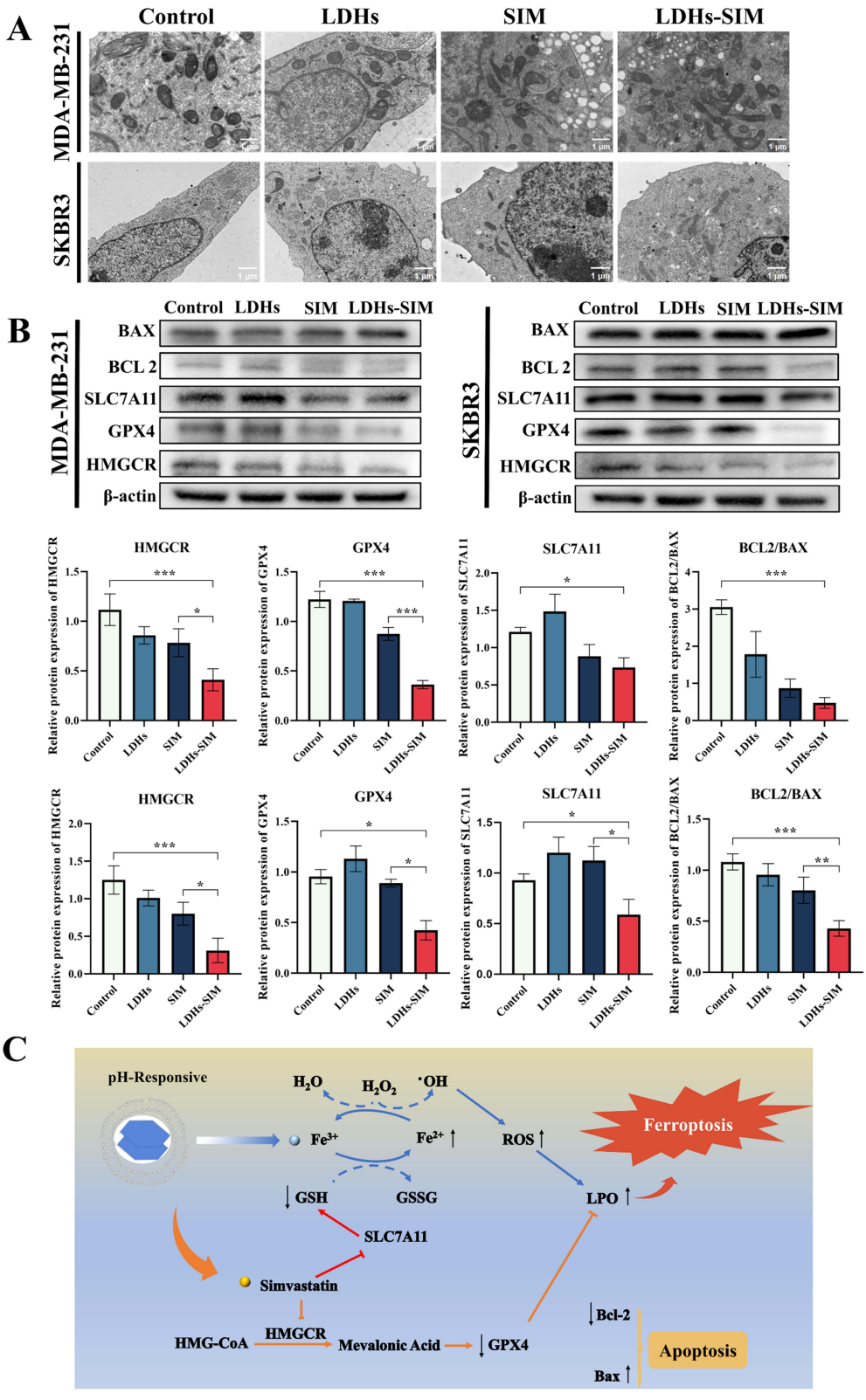

Figure 4 (**A**) Mitochondrial transmission electron microscopy images of MDA-MB-231 and SKBR3 cells treated with Control, LDHs, SIM and LDHs-SIM treatment (scale bar =1 μm). (**B**) GPX4, HMGCR, SLC7A11, Bax, Bcl-2 protein expression and quantification of MDA-MB-231 cells and SKBR3 treated with Control, LDHs, SIM and LDHs-SIM; (**C**) Schematic diagram of LDHs-SIM induced apoptosis and ferroptosis mechanisms. Data are expressed as mean ±SD, *p < 0.05, **p < 0.01, ***p < 0.001.

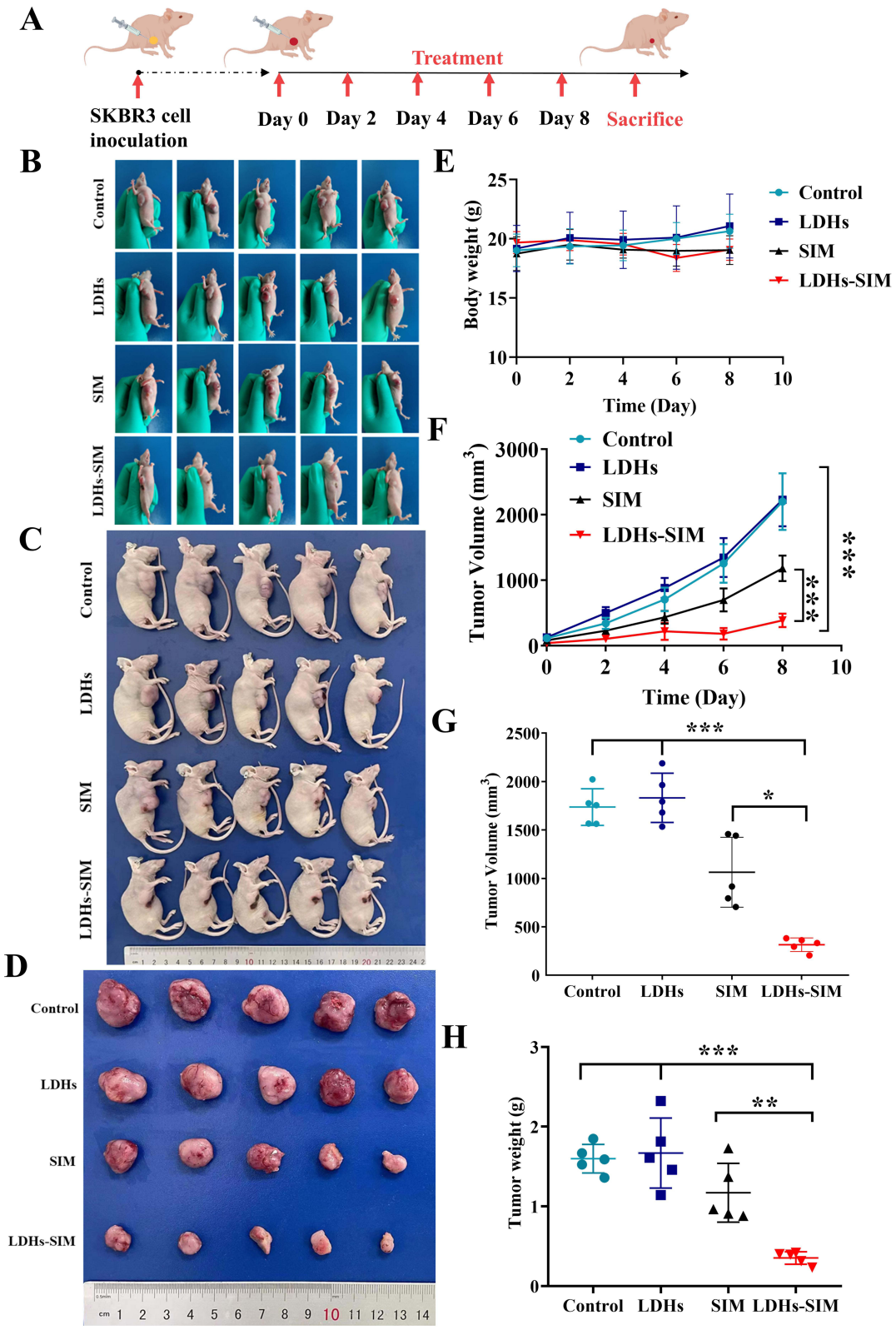

Figure 5 (**A**) Flow chart of LDHs-SIM in vivo treatment of xenograft tumors; (**B**) Pictures of subcutaneous implanted tumors in nude mice on day 8 of different treatment groups; (**C**) Tumor growth status of each treatment group after treatment; (**D**) Digital photographs of anatomical tumors in each group; (**E**) Variation of body weight curves over time in different nude mouse treatment groups; (**F**) curves of tumor volume growth over time in different treatment groups; (**G**) tumor volume after dissection of mice in each group; (**H**) Tumor weight after dissection of mice in each group. Data are expressed as mean ± standard deviation (mean ±SD) of five mice per group. *p < 0.05, **p < 0.01, ***p < 0.001.

https://doi.org/10.2147/IJN.S455427 DovePress

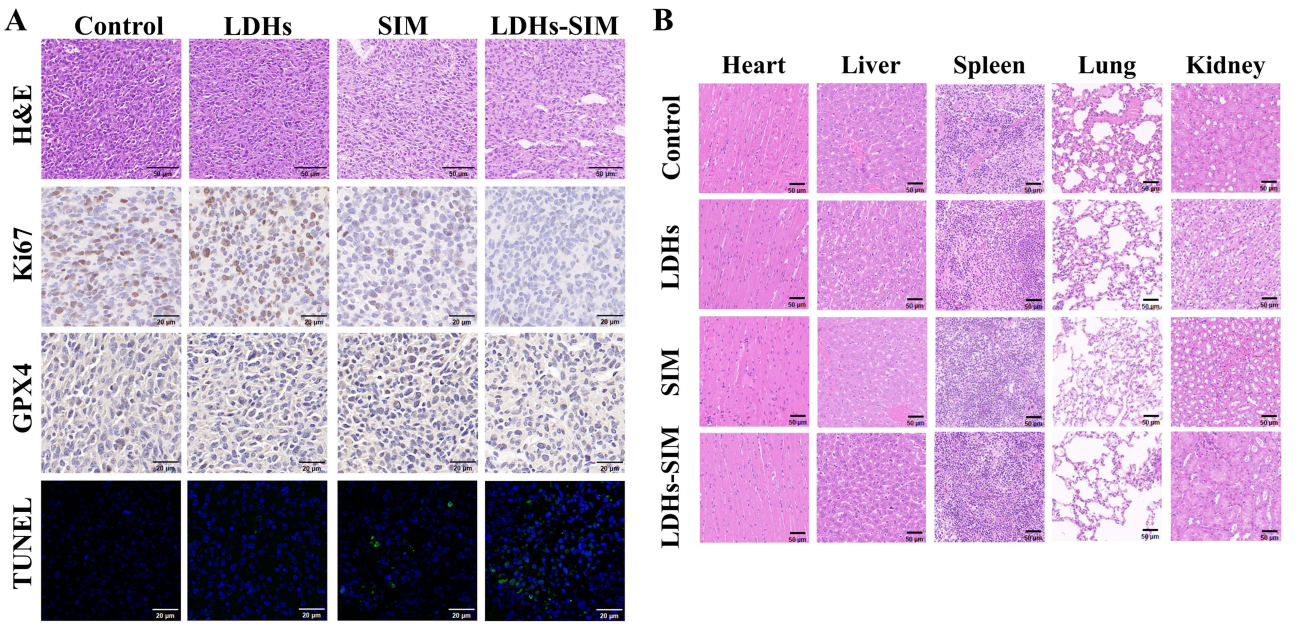

Figure 6 (**A**) H&E, ki67, TUNEL, GPX4 staining results of tumor sections in different treatment groups (scale bar = 20 μm); (**B**) H&E staining images of heart, liver, spleen, lung, kidney and other organs treated with different materials (scale bar = 50 μm).

Discussion

In view of the occurrence of metastasis and recurrence of breast cancer, new drugs are gradually being sought in clinical practice to expect the antiseptic effect of superior to chemotherapy drugs. In recent years, statins have emerged in tumor treatment and can inhibit the expression of GPX4 through the MVA pathway,[30] which is an important regulator of iron atrophy cell death,[31] so statins can promote a variety of signal transduction pathways such as ferroptosis in tumor cells to exert anti-tumor effects.[22,32] However, its characteristics of poor water solubility and rapid metabolism greatly affect the transmission and accumulation in the tumor site. With the continuous development of nanotechnology, research is committed to using nanomaterials to change the dosage form of drugs to achieve the effect of improving the efficiency of drug delivery, which undoubtedly provides great convenience for the utilization and research and development of new anti-cancer drugs.[33]

In this work, we selected simvastatin as a therapeutic drug and constructed a nanodrug-loading system using layered double hydroxides-supported SIM. The unique ionic composition and sheet structure of the layered double hydroxides we chose allow us to change the ion combination according to the purpose of the study, and the drug is easily intercalated and sustained-release. As shown in Scheme 1, this study changed the classical combination of Mg-Al ions to Mg-Fe by constructing a layered double hydroxide nanodrug carrier system loaded with simvastatin, and the effect of iron oxidation initiating ferroptosis was achieved by the addition of Fe^{3+}. LDHs are weakly alkaline materials that disintegrate in the acidic environment of tumor cells, releasing drugs and metal ions. As mentioned earlier, the content of GSH and H_2O_2 in tumor cells is high, so in breast cancer cells, the nanosystem collapses and releases Fe^{3+} in which GSH reduces Fe^{3+} to Fe^{2+}, triggering the Fenton reaction and increasing ROS content, which further acts on unsaturated fatty acids to produce LPO and induce ferroptosis. In addition, GSH depletion is a key indicator of cell-borne iron zosis.[27] At the same time, SIM inhibits GPX4 activity through the MVA pathway, and at the same time, SIM inhibits SLC7A11 expression and blocks GSH synthesis, thereby causing ferroptosis. Importantly, GPX4 knockout has been shown to induce apoptosis in glioma cells.[34] Therefore, we expect that this nanodrug-loaded system can synergize with ferroptosis and apoptosis to inhibit the occurrence of breast cancer.

In this study, we first construct and characterize the nanodrug-loaded system. After synthesis, the characteristics such as carrier size, shape, potential and stability were detected by the classic hydrothermal co-precipitation method, and whether the material was successfully constructed. The size, zeta potential and shape of the carrier are the key criteria for the success of drug delivery, and through DLS detection, the addition of SIM does not make the particle size of the material too large, and

makes the material negatively charged, ensuring stability and dispersion, making it easier to achieve drug delivery through the cell membrane. Transmission electron microscopy analysis confirmed the successful construction of LDHs-SIM. In addition, XRD and Fourier infrared spectroscopy results indicate that we constitute a material with intact crystal structure, and the retention of SIM characteristic peaks indicates successful loading of the drug.

We selected two different subtypes of breast cancer cells: MDA-MB-231 and SKBR3 cells, firstly, we preliminarily explored the cytotoxicity of free drugs and drug-loaded systems on both cells, and the cytotoxicity of the drug-loaded group was always better than that of the SIM group at different concentrations, which indicates that the nanodrug-loaded system we constructed has obvious therapeutic potential superior to SIM. In addition, the empty carrier did not exhibit cytotoxicity, and there is reason to suspect that the Fe^{3+} released by LDHs is not enough to trigger cancer cell death, on the other hand, it reflects the biological safety of the material. Use this toxicity result to determine the concentration of subsequent drug treatment. We used fluorescence photography to detect the internalization of LDHs-SIM by two types of cells intracellular localization, and the results showed that LDHs-SIM can be successfully taken up into cells within 4 hours for further action, and over time, the fluorescence intensity decreases, which may be that the drug is consumed by the action. The lysosomal escape experiment used Lysotracker to first locate the drug to lysosomes, emphasizing that the drug is captured by lysosomes, and the AO kit showed that LDHs-SIM can increase lysosomal membrane permeability and escape its capture, greatly improving the efficiency of drug action.

The following is the verification of LDHs-SIM in inducing ferroptosis in two breast cancer cells, first of all, it needs to be clear that the key factors for ferroptosis include elevated Fe^{2+} levels, excess ROS, depletion of GSH, lipid peroxidation, and insufficient expression of key protein GPX4. Based on established mechanisms of ferroptosis morbidity, we validated key indicators of ferroptosis. First, the Ferro Orange probe results showed that only LDHs and LDHs-SIM groups had significant fluorescence reactions, which verified that the nanodrug delivery system could release Fe^{3+} and reduce to Fe^{2+} in tumor cells, causing an increase in ferrous ions in tumor cells. In addition, the GSH assay kit was used to detect the corresponding levels of GSH in both cells, as excess GSH in TME may eliminate already produced ROS and maintain homeostasis required for tumor growth. The LDHs-SIM group experienced a significant decrease in intracellular GSH levels compared to other treated groups. This result suggests that LDHs-SIM nanodrug delivery systems may reduce GSH levels in tumor cells and break redox homeostasis, further amplifying the therapeutic effect. The results of flow cytometry showed that both SIM and LDHs-SIM could increase the level of ROS in breast cancer cells, but the effect of LDHs-SIM was significantly higher than that of other treatment groups. The results of Western blot showed that LDHs-SIM could significantly inhibit the protein expression of HMGCR and GPX4 in two cells, and it was verified that LDHs-SIM could release SIM to inhibit GPX4 expression through the MVA pathway, and the effect was better than that of free SIM. Members of the solute carrier family SLC7A11 are specific amino acid transporters and key regulators of ferroptosis, and down-regulation of SLC7A11 can inhibit the activity of GPX4 by inhibiting cysteine metabolic pathways, leading to reduced intracellular cystine levels and depletion of GSH biosynthesis, which in turn leads to lipid peroxide accumulation and ultimately induces ferroptosis in cells. The Western blot results showed that LDHs-SIM could downregulate the expression of SLC7A11 in both cells. As mentioned earlier, the inactivation of GPX4 inhibits the conversion of lipid peroxides to lipid alcohols and promotes the accumulation of lipid peroxide levels. It is known that ferroptosis depends primarily on an imbalance between lipid hydrogen peroxide detoxification mechanisms and lipid ROS accumulation. Excessive accumulation of lipid hydrogen peroxide activates iron toxicity and cell death. So, we think the degree of lipid peroxidation is the most reliable indicator of ferroptosis. We explored the amount of LPO in cells to assess the level of lipid peroxidation, and not surprisingly, the LPO content increased significantly after LDHs-SIM treatment. Finally, we verified by morphology that the cells had ferroptosis, and the TEM visually showed characteristic changes in the mitochondria of MDA-MB-231 and SKBR3 cells treated with LDHs-SIM, with mitochondrial membrane shrinkage, while mitochondrial crest decreased or disappeared.

It has been suggested that the progression of breast cancer is largely determined by the apoptosis of tumor cells.[21,35] Therefore, compared with pure ferroptosis induction, we hope that the nanodrug-loaded system constructed can achieve the synergy of ferroptosis and apoptosis. As mentioned earlier, low levels of GPX4 expression can lead to apoptosis, and one of the key proteins linking the two has been reported.[21] Through flow cytometry analysis, we have preliminarily defined the pro-apoptotic effect of LDHs-SIM on breast cancer cells. Further exploration by Western blot, SIM and LDHs-SIM significantly activated apoptotic protein Bax and reduced Bcl-2 levels.

In summary, as shown in Figure 4C, the mechanism by which LDHs-SIM kills breast cancer cells synergistically through ferroptosis and apoptosis can be roughly described, LDHs-SIM is internalized by breast cancer cells by endocytosis and escapes lysosomal capture, given the alkaline nature of the material, it is disintegrated by pH response in the acidic environment of tumor cells. A large amount of Fe^{3+} released will consume GSH and be reduced to Fe^{2+}, and excess ferrous ions in the cell can induce a Fenton reaction leading to the production of a large amount of ROS, which in turn induces lipid peroxidation. The collapse interpretation of the nanodrug-loaded system can release SIM by inhibiting HMGCR and then inhibiting GPX4 through the MVA pathway, and at the same time, SIM can inhibit the expression of membrane transporter SLC7A11, interfere with the synthesis of intracellular GSH, cause the depletion of intracellular GSH, and lead to the occurrence of ferroptosis.

Conclusion

In summary, this Mg-Fe-LDHs-SIM nanoparticle shows a sensitive pH-release behavior. On the one hand, the research revealed that Mg-Fe-LDHs-SIM nanoparticles could induce cell death by the ferroptosis pathway. Moreover, the detailed mechanism suggested that Mg-Fe-LDHs-SIM nanoparticles could greatly promote the synthesis of reactive oxygen species (ROS), suppress the GPX4 activity, produce lots of lipid peroxide (LPO), and thus result in enhancing the oxidative stress induced ferroptosis. On the other hand, Mg-Fe-LDHs-SIM entered the cell for induction of breast cancer cell apoptosis. The apoptosis ratio of the Mg-Fe-LDHs-SIM group was higher than those obtained with the control, LDHs and Simvastatin groups. In vitro and in vivo investigations indicate that a great therapeutic effect was achieved, suggesting that the formation of the Mg-Fe-LDHs-SIM delivery system is a promising strategy to fight against tumors by an apoptosis and ferroptosis combination modality.

Ethics Approval

The animal study was reviewed and approved by the Experimental Animal Management and Ethics Committee and Ethics Committee of Bengbu Medical University, Anhui Province, China, Ethics Number: [2023] No. 537.

Funding

This work was supported by the Nature Science Research Project of Anhui Province2108085MH294), the University Synergy Innovation Program of Anhui Province (GXXT-2022-064), the Postgraduate Research Innovation Program of Bengbu Medical College (Byycx22006) and the Anhui province Undergraduate Training Programs for Innovation and Entrepreneurship (s202310367041).

Disclosure

The authors report no conflicts of interest in this work.

References

1. Sung H, Ferlay J, Siegel RL. et al. Global cancer statistics 2020: GLOBOCAN estimates of incidence and mortality worldwide for 36 cancers in 185 countries. *CA Cancer J Clin*. 2021;71(3):209–249. doi:10.3322/caac.21660
2. Loibl S, Poortmans P, Morrow M, et al. Breast cancer. *Lancet*. 2021;397(10286):1750–1769. doi:10.1016/S0140-6736(20)32381-3
3. Benson JR, Dumitru D. Extent of breast surgery after neoadjuvant chemotherapy for triple-negative breast cancer. *JAMA Surg*. 2020;155 (8):784–785. doi:10.1001/jamasurg.2020.1001
4. Wang H, Mao X. Evaluation of the efficacy of neoadjuvant chemotherapy for breast cancer. *Drug Des Devel Ther*. 2020;14:2423–2433. doi:10.2147/DDDT.S253961
5. Yang F, Xiao Y, Ding JH, et al. Ferroptosis heterogeneity in triple-negative breast cancer reveals an innovative immunotherapy combination strategy. *Cell Metab*. 2023;35(1):84–100.e8. doi:10.1016/j.cmet.2022.09.021
6. Zhao Y, Liu ZS, Liu GQ, et al. Neutrophils resist ferroptosis and promote breast cancer metastasis through aconitate decarboxylase 1. *Cell Metab*. 2023;35(10):1688–1703.e10. doi:10.1016/j.cmet.2023.09.004
7. Bobinski R, Dutka M, Pizon M, et al. Ferroptosis, Acyl Starvation, and Breast Cancer. *Mol Pharmacol*. 2023;103(3):132–144. doi:10.1124/molpharm.122.000607
8. Dong X, Li Y, Sheng XN, et al. Mitochondria-related signaling pathways involved in breast cancer regulate ferroptosis. *Genes Dis*. 2024;11 (1):358–366. doi:10.1016/j.gendis.2023.03.019
9. Brigelius-Flohe R, Kipp A. Glutathione peroxidases in different stages of carcinogenesis. *Biochim Biophys Acta*. 2009;1790(11):1555–1568. doi:10.1016/j.bbagen.2009.03.006

10. Liang DG, Minikes AM, Jiang XJ. Ferroptosis at the intersection of lipid metabolism and cellular signaling. *Mol Cell*. 2022;82(12):2215–2227. doi:10.1016/j.molcel.2022.03.022
11. Zhang C, Liu XY, Jin SD, et al. Ferroptosis in cancer therapy: a novel approach to reversing drug resistance. *Mol Cancer*. 2022;21(1):47. doi:10.1186/s12943-022-01530-y
12. Ding Y, Chen XP, Liu C, et al. Identification of a small molecule as inducer of ferroptosis and apoptosis through ubiquitination of GPX4 in triple negative breast cancer cells. *J Hematol Oncol*. 2021;14(1):19. doi:10.1186/s13045-020-01016-8
13. Yang J, Zhou YL, Xie SD, et al. Metformin induces Ferroptosis by inhibiting UFMylation of SLC7A11 in breast cancer. *J Exp Clin Cancer Res*. 2021;40(1):206. doi:10.1186/s13046-021-02012-7
14. Xie R, Zhao W, Lowe S, et al. Quercetin alleviates kainic acid-induced seizure by inhibiting the Nrf2-mediated ferroptosis pathway. *Free Radic Biol Med*. 2022;191:212–226. doi:10.1016/j.freeradbiomed.2022.09.001
15. Fu C, Wu Y, Liu S, et al. Rehmannioside A improves cognitive impairment and alleviates ferroptosis via activating PI3K/AKT/Nrf2 and SLC7A11/GPX4 signaling pathway after ischemia. *J Ethnopharmacol*. 2022;289:115021. doi:10.1016/j.jep.2022.115021
16. Hong S, Lee Y, Lee S, et al. Treat-to-target or high-intensity statin in patients with coronary artery disease: a randomized clinical trial. *JAMA*. 2023;329(13):1078–1087. doi:10.1001/jama.2023.2487
17. Ballantyne C, Bays H, Catapano AL, et al. Role of bempedoic acid in clinical practice. *Cardiovasc Drugs Ther*. 2021;35(4):853–864. doi:10.1007/s10557-021-07147-5
18. Yang WS, Stockwell BR. Ferroptosis: death by Lipid Peroxidation. *Trends Cell Biol*. 2016;26(3):165–176. doi:10.1016/j.tcb.2015.10.014
19. Lu XY, Shi XJ, Hu A, et al. Feeding induces cholesterol biosynthesis via the mTORC1-USP20-HMGCR axis. *Nature*. 2020;588(7838):479–484. doi:10.1038/s41586-020-2928-y
20. Xie W, Peng MJ, Liu Y, et al. Simvastatin induces pyroptosis via ROS/caspase-1/GSDMD pathway in colon cancer. *Cell Commun Signal*. 2023;21(1):329. doi:10.1186/s12964-023-01359-y
21. Elakkad YE, Mohamed S, Abuelezz NZ. Potentiating the cytotoxic activity of a novel simvastatin-loaded cubosome against breast cancer cells: insights on dual cell death via ferroptosis and apoptosis. *Breast Cancer*. 2021;13:675–689. doi:10.2147/BCTT.S336712
22. Rezano A, Ridhayanti F, Rangkuyi AR, et al. Cytotoxicity of simvastatin in human breast cancer MCF-7 and MDA-MB-231 Cell Lines. *Asian Pac J Cancer Prev*. 2021;22(S1):33–42. doi:10.31557/APJCP.2021.22.S1.33
23. Gu Z, Yan SY, Cheong S, et al. Layered double hydroxide nanoparticles: impact on vascular cells, blood cells and the complement system. *J Colloid Interface Sci*. 2018;512:404–410. doi:10.1016/j.jcis.2017.10.069
24. Ameena SV, Sankar R, Johnson AP, et al. Advanced drug delivery applications of layered double hydroxide. *J Control Release*. 2021;330:398–426. doi:10.1016/j.jconrel.2020.12.041
25. Zhou J, Lei M, Peng XL, et al. Fenton reaction induced by fe-based nanoparticles for tumor therapy. *J Biomed Nanotechnol*. 2021;17(8):1510–1524. doi:10.1166/jbn.2021.3130
26. Wu F, Du YQ, Yang JN, et al. Peroxidase-like active nanomedicine with dual glutathione depletion property to restore oxaliplatin chemosensitivity and promote programmed cell death. *ACS Nano*. 2022;16(3):3647–3663. doi:10.1021/acsnano.1c06777
27. Ursini F, Maiorino M. Lipid peroxidation and ferroptosis: the role of GSH and GPx4. *Free Radic Biol Med*. 2020;152:175–185. doi:10.1016/j.freeradbiomed.2020.02.027
28. Mandal CC, Ghosh-Choudhury N, Yoneda T, et al. Simvastatin prevents skeletal metastasis of breast cancer by an antagonistic interplay between p53 and CD44. *J Biol Chem*. 2011;286(13):11314–11327. doi:10.1074/jbc.M110.193714
29. Li H, Shi W, Li XH, et al. Ferroptosis accompanied by OH generation and cytoplasmic viscosity increase revealed via dual-functional fluorescence probe. *J Am Chem Soc*. 2019;141(45):18301–18307. doi:10.1021/jacs.9b09722
30. Gaschler MM, Andia AA, Liu HR, et al. FINO(2) initiates ferroptosis through GPX4 inactivation and iron oxidation. *Nat Chem Biol*. 2018;14(5):507–515. doi:10.1038/s41589-018-0031-6
31. Xue Q, Yan D, Chen X, et al. Copper-dependent autophagic degradation of GPX4 drives ferroptosis. *Autophagy*. 2023;19(7):1982–1996. doi:10.1080/15548627.2023.2165323
32. Hao SH, Yu J, He WM, et al. Cysteine dioxygenase 1 mediates erastin-induced ferroptosis in human gastric cancer cells. *Neoplasia*. 2017;19(12):1022–1032. doi:10.1016/j.neo.2017.10.005
33. Abdel-Mageed HM, AbuelEzz NZ, Radwan RA, et al. Nanoparticles in nanomedicine: a comprehensive updated review on current status, challenges and emerging opportunities. *J Microencapsul*. 2021;38(6):414–436. doi:10.1080/02652048.2021.1942275
34. Zhao H, Ji B, Chen JG, et al. Gpx 4 is involved in the proliferation, migration and apoptosis of glioma cells. *Pathol Res Pract*. 2017;213(6):626–633.
35. Adams JM, Cory S. The Bcl-2 apoptotic switch in cancer development and therapy. *Oncogene*. 2007;26(9):1324–1337. doi:10.1038/sj.onc.1210220